# Lattice Boltzmann simulation of magnetic field effects on nanofluid

Wenning ZHOU, Yuying YAN*

*Corresponding author: Tel.: +44 (0) 115 95 13168; Fax: +44 (0) 115 95 13159; Email: yuying.yan@nottingham.ac.uk
HVACR & Heat Transfer Group, Faculty of Engineering, University of Nottingham, NG7 2RD, UK

**ABSTRACT** In this paper, the magnetic field effects on natural convection heat transfer in an enclosure filled with nanofluid are numerically investigated by using lattice Boltzmann method. The fluid in the enclosure is a water-based nanofluid containing $Al_2O_3$ nanoparticles. A uniform external magnetic field with different angles was applied. A series of simulation cases were carried out for different governing parameters including Hartmann number, Rayleigh number, the nanoparticle volume fractions and magnetic field angles. The results show that the increasing Rayleigh number and nanoparticle volume fraction improve the heat transfer in the enclosure. However, the heat transfer has been suppressed when Hartmann number increases. The results also indicate there are critical values for the Raleigh number and also the magnetic field orientation, at which the impacts of the solid volume fraction and magnetic field effects are the most pronounced.

**Keywords:** Nanofluid, Magnetic field; heat transfer; lattice Boltzmann method.

## 1. Introduction

Magnetic fluid, also known as ferrofluid, is a magnetic colloidal suspension consisting of carrier liquid and magnetic nanoparticles with typical dimensions of about 10 to 100 nm. The carrier liquids most often used are water, kerosene or various oils. The ferrofluid is a type of functional or smart fluid whose flow and energy transport processes can be controlled by adjusting an external magnetic field. Due to its distinctive characteristics, ferrofluid has been widely applied in a variety of fields such as electronic devices, mechanical engineering, aerospace, bioengineering, medical applications, and has attracted a great deal of research interests [1-3]. Many experimental and numerical works have been conducted to investigate heat transfer enhancement by nanofluid. Liu *et al.* [4] reported that with low nanoparticles concentration (1-5 vol.%), the effective thermal conductivity of the suspensions can increase by more than 20% for various mixtures. A dispersion model was employed to investigate laminar flow convective heat transfer of nanofluid in a circular tube [5]. The results clearly showed that the addition of nanoparticles to the base liquid produces considerable enhancement of heat transfer. In many industrial applications, magnetic field effects on nanofluid play a crucial role on nanofluid dynamics and heat transfer performance. Wide range of investigations has also been carried out in this area. Li *et al.* [6] conducted an experimental investigation to measure the viscosity and thermal conductivity of the magnetic fluids in either the absence or the presence of the external magnetic field. To better understand how external magnetic fields affect hear transfer of nanofluid, theoretical and numerical work has been conducted. Xuan et al. [7] numerically investigated the magnetic effects on heat transfer performance of nanofluid flowing through a micro channel. The results showed the external magnetic field can either suppress or enhance heat transfer by adjusting the orientation and magnitude of the magnetic field. Teamaha et al. [8] employed finite volume method to investigate the magnetic field effects on natural convection in square cavity. Their results indicate the heat transfer can be enhanced by increasing solid volume fraction of nanoparticles but suppressed with the increasing Hartmann numbers. The lattice Boltzmann method (LBM), which is obtaining more attention and popularity [9, 10], is applied in many areas of computational fluid dynamics, including multiphase flows [11, 12], electro-osmotic flows [13, 14], heat transfer characteristics [15, 16]. Based on a mesoscopic model which can bridge the gap between the microscopic world and the macroscopic phenomena, LBM has many advantages over conventional CFD approaches [17, 18]. Generally speaking, LBM is much easier to implement, more computationally efficient and more capable to deal with complex boundary conditions and interactions between different phases.

The purpose of the present study is to numerically investigate the natural convection of nanofluid in the presence of magnetic field with different orientations by using lattice Boltzmann method. The $Al_2O_3$/water nanofluid natural convection in an enclosure at the presence of external magnetic field with different orientations is investigated. The effects of governing parameters such as Rayleigh number, nanoparticles volume fraction, Hartmann number and the orientations of external magnetic field will be analysed.

## 2. Problem statement

The geometry of the present study is shown in figure 1. This problem considered is a natural convection in a two dimensional square cavity with sidewalls maintained at different temperatures $T_H$ and $T_L$, where $T_H > T_L$. The boundary conditions of the top and bottom walls are assumed to be adiabatic. The uniform magnetic field with constant magnitudes (Hartmann number $Ha$ = 0, 30, 60 and 90) and orientations of $\theta =$ 0°, 45°, 90°, 180° is applied. It is assumed that the induced magnetic field produced by the motion of an electrically conducting fluid is negligible compared to the applied magnetic field. The viscous dissipation and Joule heating are also neglected in this study. The enclosure is filled with $Al_2O_3$/water nanofluid which is considered to be two-dimensional, laminar and incompressible. The thermophysical properties of the nanofluid are assumed to be constant, see Table 1.

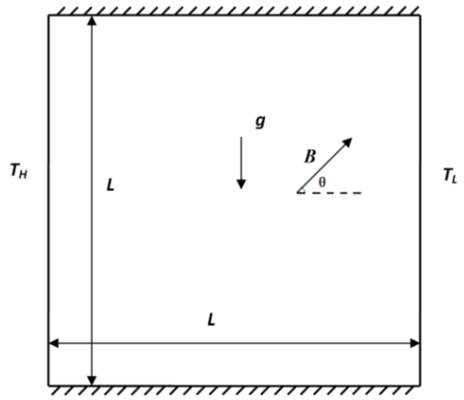


**Fig. 1: Geometry of the present study**

**Table 1 Thermophysical properties of different phases of $Al_2O_3$/water nanofluids**

| Properties | Base fluid (water) | Nanoparticles ($Al_2O_3$) |
|---|---|---|
| $\rho$ (kg/m3) | 997.1 | 3970 |
| $c_p$ (J/kg K) | 4179 | 765 |
| $\mu$ (kg/m s) | 0.001004 | / |
| $\beta \times 10^5$ (1/K) | 21 | 0.85 |
| $k$(W/m K) | 0.613 | 25 |

## 3. Methodology

### 3.1 The lattice Boltzmann method

The lattice Boltzmann method with the standard D2Q9 for the flow and temperature field is employed in this work. The details about the lattice Boltzmann method have already been given in many references [10, 19], only a brief induction will be given in this paper. The lattice Boltzmann method is carried out through two basic steps including the collision step and the streaming step, which can be written by the following form:

$$f_i(x + c_i\Delta t, t + \Delta t) = f_i(x,t) - \frac{1}{\tau}(f_i(x,t) - f_i^{eq}(x,t)) + \Delta t F_i \quad (1)$$

where $\tau$ is the dimensional relaxation time, $f_i(x,t)$ is the density distribution function for the particle moving with velocity $c_i$ at position $x$ and time $t$, and $f_i^{eq}(x,t)$ is the local equilibrium distribution function. $F_i$ is the external force term in the direction of lattice velocity. For the typical two-dimensional nine-speed (D2Q9) lattice scheme considered in the present work, the local equilibrium distribution function is defined as:

$$f_i^{(eq)} = \rho w_i [1 + \frac{c_i \cdot u}{c_s^2} + \frac{(c_i \cdot u)^2}{2c_s^4} - \frac{u \cdot u}{2c_s^2}], \qquad (2)$$

where $w_i$ is weighting factor, given as 4/9 for $i$ =0, 1/9 for $i$ =1,2,3,4, and 1/36 for $i$ =5,6,7,8. $c_s$ is the sound speed. $c_i$ is the discrete velocities, and defined as:

$$c_i = \begin{cases} (0,0), i = 0 \\ c(\cos\theta_i, \sin\theta_i), (\theta_i = (i-1)\pi/2, i = 1,2,3,4) \\ \sqrt{2}c(\cos\theta_i, \sin\theta_i), (\theta_i = (i-5)\pi/2 + \pi/4, i = 5,6,7,8) \end{cases} ,(3)$$

where $c = \Delta x / \Delta t$ is the particle streaming speed. $\Delta x$ , $\Delta t$ are the lattice spacing and time step. The relation between $c_s$ and $c$ can be expressed as $c_s = c/\sqrt{3}$ . The macroscopic variables such as the mass density, the momentum density and the pressure are defined by sums over the distribution functions:

$$\rho = \sum_i f_i \,,\; \rho u = \sum_i f_i c_i \,,\; p = \frac{c^2}{3}\rho \qquad (4)$$

The kinematic viscosity is determined by:

$$\nu = (\tau - 1/2)c_s^2 \Delta t \qquad (5)$$

For the scalar function (temperature in this study), another distribution is defined as:

$$g_i(x + c_i\Delta t, t + \Delta t) = g_i(x,t) - \frac{1}{\tau}(g_i(x,t) - g_i^{eq}(x,t)) \qquad (6)$$

The equilibrium distribution function can be written as:

$$g_i^{(eq)} = w_i T[1 + \frac{c_i \cdot u}{c_s^2}] \qquad (7)$$

The macroscopic temperature is calculated as follow:

$$T = \sum_i g_i \qquad (8)$$

The thermal diffusivity is related to the relaxation time by:

$$\alpha = (\tau_c - 1/2)c_s^2 \Delta t \qquad (9)$$

For natural convection, the important dimensionless parameters Prandtl number *Pr* and Rayleigh number *Ra* are defined as:

$$\Pr = \nu / \chi \qquad (10)$$

$$Ra = g\beta \Delta T L^3 \Pr / \nu^2 , \qquad (11)$$

where $\Delta T$ is the temperature difference between the high temperature wall and low temperature wall. $L$ is the characteristic length of the square cavity.

Another dimensionless parameter Mach number *Ma* is defined as:

$$Ma = u_c / c_s \;, \qquad (12)$$

where $u_c = \sqrt{g\beta \Delta T L}$ is the characteristic velocity of natural convection. Considering LBE applies in incompressible limit, Mach number should be less than 0.3. In present study, Mach number was fixed at *Ma*=0.1.

In the simulation the Boussinesq approximation is applied to the buoyancy force term. It that case, the buoyancy force term is added as:

$$F_i = 3 w_i \rho g \beta \Delta T \qquad (13)$$

The effect of the external magnetic field influences only the force term where a new parameter is added to the buoyancy force term:

$$F_i = F_{ix} + F_{iy} \qquad (14)$$

$$F_{ix} = 3 w_i \rho [A(v \sin\theta \cos\theta - u \sin^2\theta)] \qquad (15)$$

$$F_{iy} = 3 w_i \rho [g\beta \Delta T + A(u \sin\theta \cos\theta - v \cos^2\theta)] \qquad (16)$$

In the lattice Boltzmann model, real quantities such as space and time need to be converted to lattice units prior to simulation. By introducing characteristic scales, the dimensionless process can be accomplished. To make sure that the simulation case represents the relevant practical phenomenon, non-dimensional quantities such as Reynolds number remain the same in the dimensionless process.

3.2 **Lattice Boltzmann model for nanofluid**

In this study, the nanofluid is assumed similar to a single phase fluid. Hence, the equations of physical parameters of the nanofluid are as follows:

Density equation:

$$\rho_{nf} = (1-\phi)\rho_f + \phi\rho_p \tag{17}$$

where $\rho_{nf}$ is the density of nanofluid, $\rho_f$ is the density of base fluid and $\rho_p$ is the density of nanoparticle. $\phi$ is the volume fraction of nanoparticles.

Heat capacity equation is expressed by:

$$(\rho c_p)_{nf} = (1-\phi)(\rho c_p)_f + \phi(\rho c_p)_p \tag{18}$$

and the dynamic viscosity equation is given by:

$$\mu_{nf} = \mu_f /(1-\phi)^{2.5} \tag{19}$$

The thermal expansion coefficient of the nanofluid can be calculated by:

$$(\rho\beta)_{nf} = (1-\phi)(\rho\beta)_f + \phi(\rho\beta)_p \tag{20}$$

The effective thermal conductivity of the nanofluid can be determined by the Maxwell-Garnett (MG) model by:

$$\frac{k_{nf}}{k_f} = \frac{k_p + 2k_f - 2\phi(k_f - k_p)}{k_p + 2k_f + \phi(k_f - k_p)} \tag{21}$$

The local Nusselt number and the average value at the hot and cold walls are calculated as:

$$Nu_y = -\frac{L}{\Delta T}\frac{\partial T}{\partial x} \tag{22}$$

$$Nu_{avg} = \frac{1}{L}\int_0^H Nu_y dy \tag{23}$$

where $L$ is the height of the square, $\Delta T$ is temperature difference between the hot and cold walls. For the convenience, a normalized average Nusselt number is defined as the ratio of Nusselt number at any volume fractions of nanoparticles to that of pure water is as follows:

$$Nu^*_{avg}(\varphi) = Nu_{avg}(\varphi) / Nu_{avg}(\varphi = 0) \tag{24}$$

3.3 **Boundary treatments**

The implementation of boundary conditions is very important for LBM simulations. The unknown distribution functions pointing to the fluid zone at the boundary nodes must be specified after every iteration step. Concerning the no-slip boundary condition, bounce back boundary condition is employed on the solid boundaries.

The top and bottom of the boundaries are adiabatic so bounce back boundary condition is employed. Temperatures at the left and right walls are known. Since we are using D2Q9, for the left wall, the unknown distribution functions are evaluated as:

$$\begin{aligned} g_1 &= T_H(w(1)+w(3)) - g_3 \\ g_5 &= T_H(w(5)+w(7)) - g_7 \\ g_8 &= T_H(w(8)+w(6)) - g_6 \end{aligned} \tag{25}$$

The unknown distribution functions can be obtained in the similar way at the right wall.

## 4. Validation and gird independence

An extensive mesh testing procedure was firstly conducted to ensure grid independence. Calculations of different mesh cases were carried out for 4% $Al_2O_3$/water nanofluid of $Ra$=1×10$^4$, 1×10$^5$ and 1×10$^6$, respectively. The average Nusselt numbers were calculated and the grid independence is ensured which can be seen in Fig. 2. It can be seen that the lattice number has a positive impact to the viscosity in the lattice Boltzmann model. To keep the relaxation times in a suitable range for both flow dynamics and thermal evolution in lattice

Boltzmann model, the lattice number is particularly considered and different meshes for different cases are also considered. In the present study, 100×100 lattices is chosen for Rayleigh number is less than $1\times10^5$ and 150×150 lattices for the others cases.

To further validate the proposed lattice Boltzmann model for incompressible fluid, the simulation results were compared not only with the experimental results of Krane and Jessee [20] but also numerical work by Khalil Khanafer *et al.* [21] for natural convection in an enclosure filled with air. Fig. 3 shows that the comparisons are in excellent agreement.

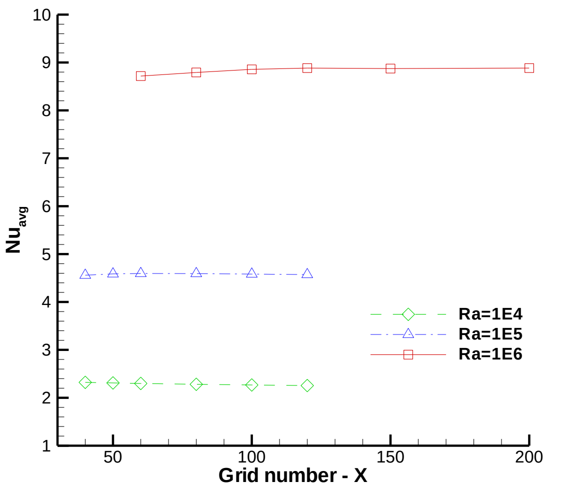


**Fig. 2: Grid independent test: $Nu_{avg}$ versus grid number (4% $Al_2O_3$/water nanofluid)**

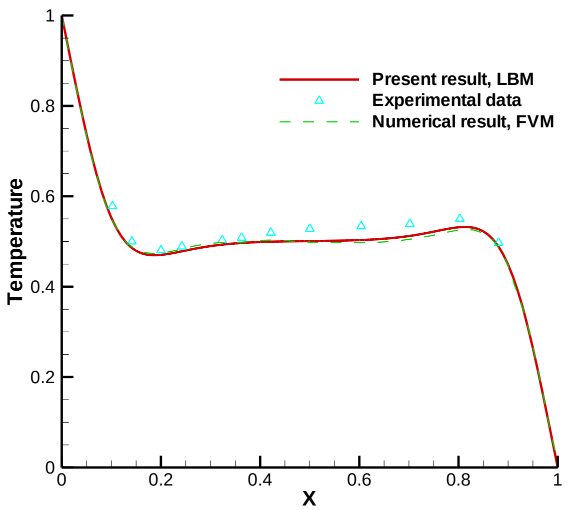


**Fig. 3: Comparison with other simulation and experimental results (*Ra*=$1.89\times10^5$, *Pr*=0.71)**

## 5. Results and discussion

To investigate the effects of the governing parameters including Hartmann number, Rayleigh number, the nanoparticle volume fractions and magnetic field angles on the heat transfer performances, a series of simulation cases were carried out with the governing parameters, Rayleigh number ranging from $1\times10^3$ to $1\times10^6$, solid volume fraction 0 to 5%, Hartmann number 0 to 90 and magnetic field orientation from 0° to 180°.

Fig. 4 shows the effect of Rayleigh number on the isotherms of the nanofluid ($\varphi = 0.04$). It can be seen that by the increasing of Rayleigh number, the effect of the convective heat transfer becomes more significant and the thickness of thermal boundary layer near the wall decreases. The effect of Rayleigh number on the temperature distribution at x-direction of the enclosure can be found in Fig. 5. When Rayleigh number is larger than $1\times10^5$, the temperature near the heated wall decreases significantly. As Rayleigh number decreases, a more gradual decrease of the temperature has been found.

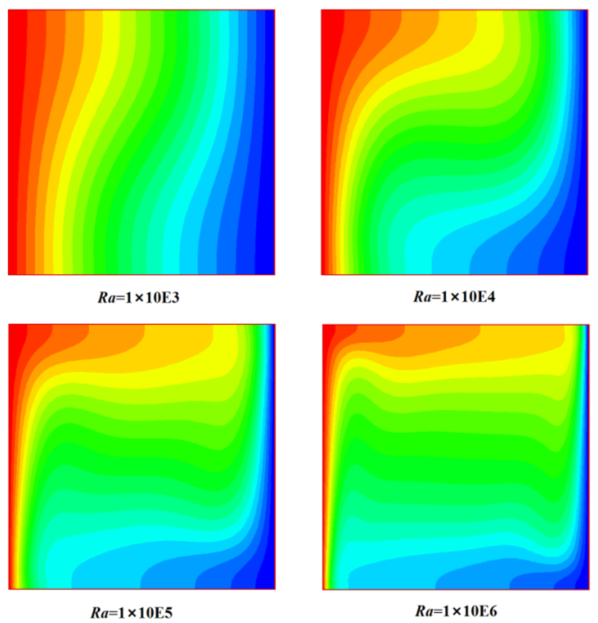


**Fig. 4: The effects of Rayleigh number on the isotherms ($\varphi = 0.04$)**

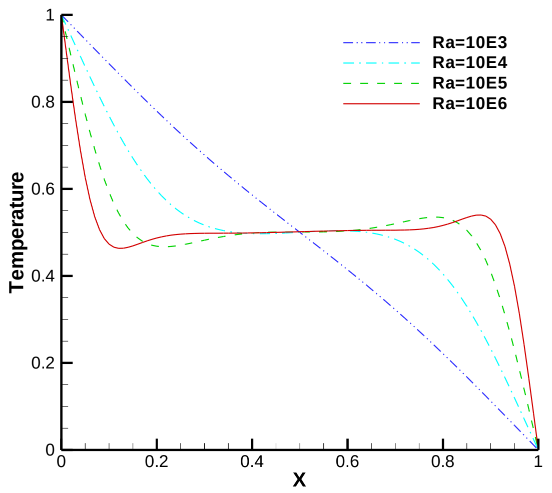


**Fig. 5: The effects of Rayleigh number on the temperature distribution at y=0.5 ($\varphi = 0.04$)**

Fig. 6 shows the effect of nanoparticle volume fraction on the heat transfer. It can be seen from the figure that with the increase in volume fraction, the isotherms become closer to the vertical wall. The thermal layer becomes thinner compared with the pure fluid. It is observed that the increase of solid concentration leads to the enhancement of heat transfer, and such enhancement is due to the increase of the effective thermal conductivity with the increase of solid volume fractions of nanoparticles.

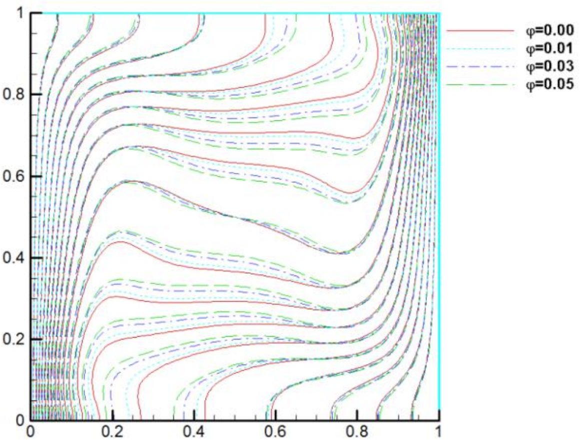


**Fig. 6: Comparison of isotherms between base fluid and nanofluid at $Ra$=1×10$^5$**

Fig. 7 presents the comparisons between the pure fluid and nanofluid of the local Nusselt number distribution along the heated wall. It can be seen that the increase of volume fractions increases the local Nusselt number along the heated wall. The influence is more evident at the bottom of the hot wall.

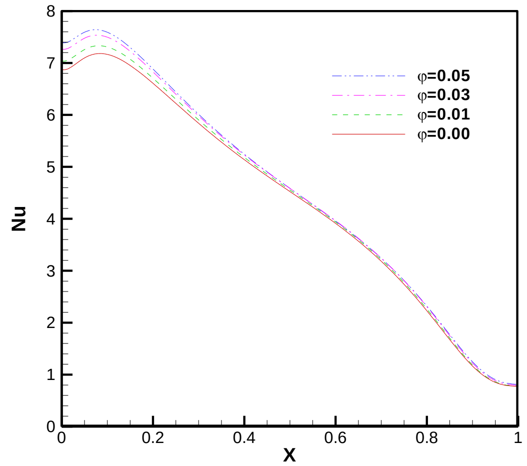


**Fig. 7: The effects of volume fractions on the local Nusselt number along the hot wall ($Ra$=1×10$^5$)**

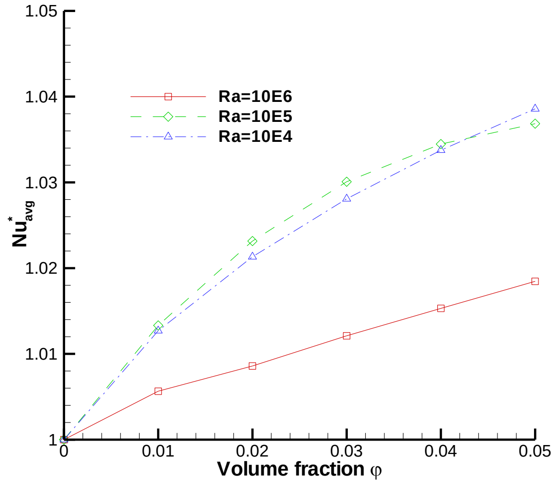


**Fig. 8: The effects of volume fractions on the normalized Nusselt number**

Fig. 8 shows the effect of volume fractions on the normalized average Nusselt number. It is worth mentioning that for a fixed Rayleigh number, solid volume fractions can affect the enhancement of heat transfer. However the effect decreases with the increase of Rayleigh number. By adding 5% $Al_2O_3$ nanoparticles by volume, the normalized Nusselt number increases about 3.8% at $Ra$=1×10$^4$, a slight decline to 3.5% at $Ra$=1×10$^5$, but decreases significantly to 1.6% when Rayleigh number increases to 1×10$^6$. This means that there is a critical value of Rayleigh number of $Al_2O_3$/water nanofluid for the performance of heat transfer enhancement in terms of the normalized average Nusselt number. Similar conclusion was obtained in [22].

Fig. 9 shows the effect of Hartmann number on the Nusselt number. As Hartmann number increases the Nusselt number decreases for constant Rayleigh number. When applying an external magnetic field on the enclosure, the velocity field suppresses owing to the retarding effect of the Lorenz force. Therefore, the convective heat transfer weakens dramatically.

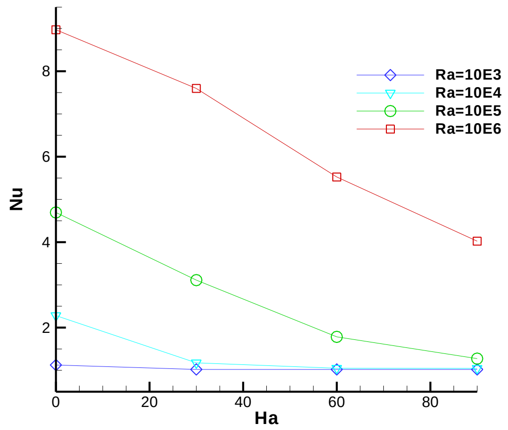


**Fig. 9: The effects of Hartmann number on the Nusselt number ($\varphi = 0.04$)**

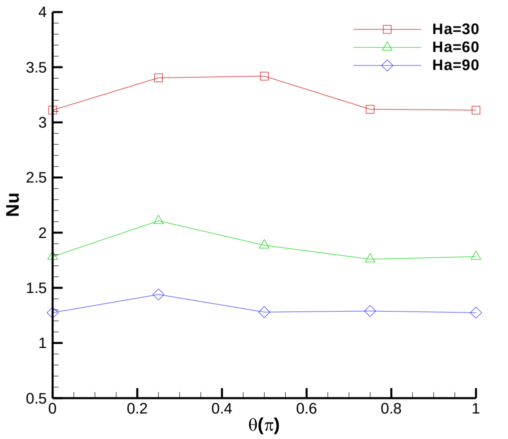


**Fig. 10: The effects of magnetic field direction on Nusselt number ($Ra$=1×10$^5$, $\varphi = 0.04$)**

Fig. 10 shows the effects of magnetic field orientation, see Fig. 1, on the average Nusselt number. It is found that for a fixed Rayleigh number and volume fraction, the average Nusselt number has a slight rise from 0° to 45°($\theta = 0.25\pi$) then declines regularly with the increasing orientation. This means there is a critical value of the magnetic field orientation at which the magnetic field has most pronounced effect for natural convection.

## 6. Conclusions

In the present paper, the effects of a magnetic field on natural convection heat transfer in an enclosure filled with nanofluid have been investigated by employing the lattice Boltzmann method. The effects of Rayleigh number, nanoparticle volume fraction, Hartmann number and magnetic field orientation on the characteristics of flow and heat transfer have been examined. The following conclusions can be drawn:

(1) The increase of volume fraction of the suspended $Al_2O_3$ nanoparticles in pure water enhances the heat transfer in the enclosure at various Rayleigh numbers. However, there is a critical Rayleigh number for heat transfer enhancement of applying nanofluids; beyond the critical value, the enhancement rate will be reduced.

(2) The average Nusselt number and normalized average Nusselt number increase with the volume fractions of nanoparticles and also Rayleigh number.

(3) The heat transfer coefficient of nanofluid decreases with the increase of Hartmann number for a fixed Rayleigh number and nanoparticle volume fraction. The effect of Hartmann number is more pronounced at higher Rayleigh number.

(4) For various Hartmann numbers, a critical magnetic field orientation, i.e. $\theta = 0.25\pi$ , has been noted, at which the magnetic field has the most pronounced effect.

## Acknowledgements

This work is supported by the scholarship joint sponsored by the University of Nottingham, UK and Chinese Scholarship Council (CSC), also by Royal Society-NSFC joint project under IE110858 (2012-2014).

## References

[1] Pankhurst Q.A., Connolly J., Jones S., Dobson J., Applications of magnetic nanoparticles in biomedicine, Journal of physics D: Applied physics, 36 (2003) R167.

[2] Jordan A., Scholz R., Maier-Hauff K., Johannsen M., Wust P., Nadobny J., Schirra H., Schmidt H., Deger S., Loening S., Presentation of a new magnetic field therapy system for the treatment of human solid tumors with magnetic fluid hyperthermia, J Magn Magn Mater, 225 (2001) 118-126.

[3] Ruuge E., Rusetski A., Magnetic fluids as drug carriers: targeted transport of drugs by a magnetic field, J Magn Magn Mater, 122 (1993) 335-339.

[4] Liu M.S., Ching-Cheng Lin M., Huang I., Enhancement of thermal conductivity with carbon nanotube for nanofluids, Int Commun Heat Mass, 32 (2005) 1202-1210.

[5] Heris S.Z., Esfahany M.N., Etemad G., Numerical investigation of nanofluid laminar convective heat transfer through a circular tube, Numerical Heat Transfer, Part A: Applications, 52 (2007) 1043-1058.

[6] Li Q., Xuan Y., Wang J., Experimental investigations on transport properties of magnetic fluids, Experimental Thermal and Fluid Science, 30 (2005) 109-116.

[7] Xuan Y., Li Q., Ye M., Investigations of convective heat transfer in ferrofluid microflows using lattice-Boltzmann approach, Int J Therm Sci, 46 (2007) 105-111.

[8] Teamah M.A., El-Maghlany W.M., Augmentation of natural convective heat transfer in square cavity by utilizing nanofluids in the presence of magnetic field and uniform heat generation/absorption, Int J Therm Sci, 58 (2012) 130-142.

[9] Yan Y.Y., Zu Y.Q., Dong B., LBM, a useful tool for mesoscale modelling of single-phase and multiphase flow, Appl Therm Eng, 31 (2011) 649-655.

[10] Chen S., Doolen G.D., Lattice Boltzmann method for fluid flows, Annu Rev Fluid Mech, 30 (1998) 329-364.

[11] Zu Y., Yan Y., Li J., Han Z., Wetting Behaviours of a Single Droplet on Biomimetic Micro Structured Surfaces, Journal of Bionic Engineering, 7 (2010) 191-198.

[12] Yan Y.Y., Zu Y.Q., A lattice Boltzmann method for incompressible two-phase flows on partial wetting surface with large density ratio, J Comput Phys, 227 (2007) 763-775.

[13] Li B., Zhou W., Yan Y., Han Z., Ren L., Numerical Modelling of Electroosmotic Driven Flow in Nanoporous Media by Lattice Boltzmann Method, Journal of Bionic Engineering, 10 (2013) 90-99.

[14] Li B., Zhou W.N., Yan Y.Y., Tian C., Evaluation of electro-osmotic pumping effect on microporous media flow, Appl Therm Eng, 60 (2013) 449-455.

[15] Kefayati G.R., Hosseinizadeh S.F., Gorji M., Sajjadi H., Lattice Boltzmann simulation of natural convection in tall enclosures using water/SiO2 nanofluid, Int Commun Heat Mass, 38 (2011) 798-805.

[16] Xuan Y.M., Yao Z.P., Lattice Boltzmann model for nanofluids, Heat Mass Transfer, 41 (2005) 199-205.

[17] Aidun C.K., Clausen J.R., Lattice-Boltzmann Method for Complex Flows, Annu Rev Fluid Mech, 42 (2010) 439-472.

[18] Begum R., Basit M.A., Lattice Boltzmann Method and its Applications to Fluid Flow Problems, European Journal of Scientific Research, 22 (2008) 216-231.

[19] He X., Luo L.S., Theory of the lattice Boltzmann method: From the Boltzmann equation to the lattice Boltzmann equation, Phys Rev E, 56 (1997) 6811-6817.

[20] Krane R., Jessee J., Some detailed field measurements for a natural convection flow in a vertical square enclosure, in: Proc. 1st ASME-JSME Thermal Engineering Joint Conf, 1983, pp. 323-329.

[21] Khanafer K., Vafai K., Lightstone M., Buoyancy-driven heat transfer enhancement in a two-dimensional enclosure utilizing nanofluids, Int J Heat Mass Tran, 46 (2003) 3639-3653.

[22] Dellar P.J., Lattice kinetic schemes for magnetohydrodynamics, J Comput Phys, 179 (2002) 95-126.